Original Article

Assessment of Single-and Double-Strand Breaks in DNA Induced by Auger Electrons of Radioisotopes Used in Diagnostic and Therapeutic Applications

Mahdi Seifi Moradi, Babak Shirani Bidabadi

Department of Nuclear Engineering, Faculty of Physics, University of Isfahan, Isfahan, Iran

Abstract

Introduction: Most of the radionuclides that are used for diagnostic purposes emit Auger electrons and can thus cause damage to the DNA molecule on a nanometer scale. Therefore, the nanodosimetric calculation of these radioisotopes is necessary to achieve better understanding on their effects. **Aim:** The aim of this study was to calculate the mean number of DNA strand breaks (single-strand breaks and double-strand breaks) caused by direct and indirect effects for six widely used Auger electron-emitting diagnostic radioisotopes, including ^{123}I, ^{125}I, ^{99m}Tc, ^{67}Ga, ^{201}Tl, ^{111}In and two therapeutic radioisotopes of ^{131}I(beta + Auger + CK emitter) and ^{211}At(alpha + Auger + CK emitter). **Materials and Methods:** Geant4-DNA simulation tool was used to evaluate the effects of Auger electrons, beta and alpha particles of these radioisotopes on DNA molecules. Two different DNA molecule geometric models were simulated and the results of these two models were compared with each other as well as with the results of previous studies. **Results and Conclusion:** The results showed that the geometric shape of the sugar-phosphate groups may have a significant effect on the number of single-strand breaks (SSBs) and double-strand breaks (DSBs) of the DNA molecule. Among the most widely used diagnostic radioisotopes, ^{201}Tl and ^{125}I, had the greatest impact on the number of SSBs and DSBs, respectively, while therapeutic radioisotope of ^{131}I almost had no effect, therapeutic radioisotope of ^{211}At had the moderate effect on the number of breaks in the DNA chain.

Keywords: Auger electron, DNA molecule, double-strand breaks, Geant4-DNA, single-strand breaks

Received on: 31-08-2019 **Review completed on: 02-12-2020** **Accepted on: 02-12-2020** **Published on: 02-02-2021**

Introduction

A number of widely-used diagnostic radioisotopes are Auger electron-emitter, most of which, due to having short range in tissue; from a few nanometers to micrometers; low energy; and medium LET, can have significant effects on living cells on a nanoscale. Considering the above characteristics, these radioisotopes can produce high levels of toxicity in cancer cells and are therefore suitable for use in molecularly targeted radiotherapy (MTRT).[1,2] Due to the short range of these electrons and their energy transfer at the site of decay, there is minimal irradiation of healthy cells adjacent to cancerous cells and therefore absorbed dose of healthy cells decreases.

A number of radioisotopes used in nuclear medicine have been proposed for molecular radiotherapy of some small metastases in cancer cells.[3-5] ^{123}I Radioisotope, as an Auger electron emitter, can be used to treat certain types of cancer.[6] For this purpose, IdUrd drug (Thymidine analogue 5-iodo-2'-deoxyuridine), which carries ^{123}I and will be located on the thymidine base of DNA molecule was used by Stigbrand *et al*.,[6] and Pomplun.[7]

Watanabe *et al*.,[8] and Faraggi *et al*.,[9] also confirmed that Auger electron emitters have the potential for targeted-radiotherapy when they are located near the target site. Internal conversion electrons (even when decay occurs in the nucleoplasm) may also reach the cell's nucleus and cause damage to the DNA molecule Faraggi *et al*.[9] They calculated the dose rate of

Address for correspondence: Dr. Babak Shirani Bidabadi, Faculty of Physics, University of Isfahan, Isfahan, Iran.
E-mail: b.shirani@ast.ui.ac.ir

Access this article online

Quick Response Code:

Website: www.jmp.org.in

DOI: 10.4103/jmp.JMP_79_19

How to cite this article: Moradi MS, Bidabadi BS. Assessment of single-and double-strand breaks in DNA induced by auger electrons of radioisotopes used in diagnostic and therapeutic applications. J Med Phys 2020;45:240-8.

a number of Auger electron-emitting radionuclides on a micrometer scale and in spherical cells with size of large lymphocytes. They concluded that the dose rate is highly dependent on the intracellular distribution of radioisotopes. When ^{99m}Tc, ^{123}I, ^{111}In, ^{67}Ga, and ^{201}Tl radioisotopes are distributed in the cell nucleus, the rate of absorbed dose at the nucleus is 94, 21, 18, 74, and 76 times higher than the state in which these radioisotopes are distributed in the cell membrane.

In addition to having the potential to be used in cell treatment, Auger electron-emitting diagnostic radioisotopes may also damage the DNA molecule because of their short-range. Therefore, it is necessary to make a comprehensive assessment of their effects and their damage to the DNA. The DNA molecule is composed of two strands running opposite to each other and connected by hydrogen bonding and forming a binary spiral structure. Each strand is a linear chain of 4 bases of adenine, cytosine, guanine and thymine linked by sugar molecules and forming sugar-phosphate backbone.

Two major damages that can occur in the DNA molecule include single-strand break (SSB) and double-strand break (DSB).[10,11] These breaks can be due to the direct ionization of the DNA molecule by ionizing radiation (direct effects) or by the interaction of water-based active radicals with the DNA molecule (indirect effects).

Tounekti *et al*.,[12] studied the relationship between types of cell death and number of SSBs and DSBs of DNA molecules for Chinese hamster fibroblasts using different experimental endpoints and applying bleomycin (Bleomycin) and deglyco-bleomycin antibiotics, which induced SSBs and DSBs in DNA molecules. They considered three types of cell death, namely apoptosis, mitotic cell death as pseudoapoptosis as well as repair for cells, according to the type and number of strand breaks of the DNA molecule. For example, they concluded that cell death can occur as apoptosis in case of 150000 <SSBs and 500 <DSBs; in contrast, if the number of SSBs and DSBs is smaller than 150,000 and 500, respectively, cell death does not occur and the repair process occurs instead. These threshold values for other cells can vary, which depends on the potential for DNA repair of other cells, and these thresholds cannot be used with certainty for all cells.

In a study, Pomplun[7] used MOCA8b code to evaluate DNA molecule chain breaks caused by direct effects of decay of ^{123}I and ^{125}I radioisotopes. He calculated Auger electron-induced the number of SSBs and DSBs caused by ^{123}I as 1.1 and 0.2, and by ^{125}I as 1.9 and 0.4, per decay respectively. So far, different geometric models and various Monte Carlo codes have been used to evaluate the DNA chain breaks caused by the Auger electrons. In previous studies, linear DNA models in the form of small cylinders (smaller than 100 nm) representing duplex, nucleosome, and chromatin fibers of the DNA molecule have been used to calculate the absorbed energy.[13]

Nikjoo *et al*.,[13] traced the Auger electrons produced by the characteristic soft X-rays of C (278 eV), Al (1487 eV) and Ti (4509 eV) elements, using the Monte Carlo technique (MOCA8b code) and calculated the amount of absorbed energy in cylinders with a diameter of 1-100 nm. The results showed that for a constant diameter, by increasing in cylinder length, the amount of absorbed energy increased slowly. A comparison was also made between the absorption of the energy produced by the above-mentioned characteristic X-rays with the energies of 1.2 MeV and 300 kV particle beams (particles with high LET) and 100 kV electron beams (particles with low LET) in small target volumes. The results showed that characteristic soft X-rays are more effective in comparison with other high-and low-LET radiations in transmitting and absorbing the energy in nano-sized volumes.

The volumetric DNA model was developed by Charlton and Humm.[14] This model was simulated in a cylindrical shape with a diameter of 2.3 nm, divided into three smaller cylindrical volumes. One of these volumes was a central cylinder of diameter of 1 nm, indicating the volume occupied by base pairs. Two other volumes included semi-cylindrical shells of height of 0.34 nm, internal radius of 0.5 nm, and external radius of 1.5 nm, which surrounds the central cylinder and represents the volume occupied by sugar-phosphate backbone. Ftacnikova and Bohm[15] and Humm and Charlton[16] used this model to count the DNA molecule breaks. In their study, Ftacnikova and Bohm[15] calculated the number of SSBs caused by direct effects of the Auger electrons per decay using the ETRACK code for the ^{123}I, ^{125}I, ^{67}Ga, $^{99\ m}$Tc, and ^{77}Br radioisotopes as 0.72, 1.18, 0.39, 0.57 and 0.46, respectively and the number of DSB for ^{125}I as 0.73.

Using the MOCA7b code, Charlton and Humm[14] calculated the number of DSBs of the DNA molecule caused by the Auger electrons of two different spectra of the ^{125}I radioisotope as 0.90 and 0.65 per decay, respectively. They also concluded that at least 100 eV energy was needed to cause a significant damage to the DNA molecule.

Friedland *et al*.,[17] and Friedland *et al*.,[18] using PARTRAC code showed by increasing the distance between two SSBs for being scored as a DSB from 2 to 10 bp enhanced the DSB yield almost by a factor of 3. Furthermore, DSB yield increases with increasing LET. For heavier ions (B, C, N, O, Ne, S), the DSB yields are lower than for helium ions of the same LET.

It is 17 years after presenting of the atomic model by Pomplun,[7] another volumetric model of the DNA molecule was used by Bernal and Liendo.[19] The same model was also used by Raisali *et al*.,[20] and Semsarha *et al*.[21]

Bernal and Liendo[19] evaluated the ability of PENELOPE code in nano-dosimetry calculation for a number of radioisotopes using this model. The calculated SSB and DSB values were 20%–76% and 50%–60% lower than those reported in other studies. They attributed this significant decline to the inability of PENELOPE code in tracing low-energy electrons and they proposed that the energy range of PENELOPE code must be

expanded up to 10 eV energy in order to calculate DNA damage caused by the electrons.

Raisali *et al*.[20] used this volumetric model and used the Geant4 code to calculate the Auger electrons-induced SSBs and DSBs after exposure to ^{123}I and ^{125}I radioisotopes.

Considering the foregoing, the Auger electrons are capable of causing damage to the cells and DNA molecules. Therefore, a comprehensive dosimetry assessment must be carried out on the Auger electrons.

Using Geant4-DNA, calculation of SSBs and DSBs caused by low energy electrons were performed by Raisali *et al*.,[20] (Auger electrons of ^{123}I and ^{125}I) and Semsarha *et al*.,[21] (Monoenergetic electrons 1-20 keV). In the present study, dosimetry calculations were performed to evaluate the number of SSBs and DSBs occurring by radioisotopes commonly used in nuclear medicine including ^{123}I, ^{125}I, $^{99\,m}$Tc, ^{67}Ga, ^{201}Tl and ^{111}In, as well as two therapeutic radioisotopes of ^{131}I and ^{211}At on a nanometer scale using Geant4-DNA simulation tool. Despite the lack of information, for some of the radioisotopes the results were compared with the results of other codes as well as the experimental measurements.

The selected radioisotopes have been widely used in the diagnosis and treatment of diseases. ^{201}Tl is used for assessing heart function such as assessing cardiac systolic function and predicting prognosis in patients with cardiovascular disease.[22] ^{123}I is the most suitable isotope of iodine for the diagnostic study of thyroid diseases. Recently it was used to identify myocardial sympathetic denervation patterns in patients with Parkinson's disease.[23] ^{99m}Tc is used for imaging and functional studies of brain, myocardium, thyroid, lungs, liver, gallbladder, kidneys, skeleton, blood, and tumors. Approximately 85% of diagnostic imaging procedures in nuclear medicine use this isotope as radioactive tracer.[24] ^{111}In can be used to bind antibodies, peptides, other targeted molecules or cells for imaging and treating cancers.[24] ^{67}Ga is used to image inflammation, chronic infections and tumors. Recently, it was used for detecting infected lower limb prostheses.[25] ^{125}I has uses in biological assays, nuclear medicine imaging and in radiation therapy as brachytherapy to treat a number of conditions, including prostate cancer, uveal melanomas, and pediatric skull base tumors.[26] ^{131}I can be used in medical therapies as a treatment tool. It is most commonly used in the treatment of hyperthyroidism due to Graves disease or a nodule in the thyroid gland.[24] ^{211}At has the most prospective as an alpha emitter for targeted radiotherapy such as treatment of compartmental tumors.[24]

The present study also used two new volumetric model, which are similar to the volumetric model presented by Raisali *et al*.,[20] and Semsarha *et al*.[21] Two different geometric shapes were considered for the sugar-phosphate groups in the DNA molecule in these two models. The credibility of these simple volumetric models has been confirmed by simulation results, experimental results, and the results of the atomic model proposed by Pomplun.[7] Therefore, these models can be used to reduce the computational time without compromising the accuracy of calculations compared to atomic models, which have more details. Other innovations in this study are the calculation of SSBs and DSBs due to widely-used Auger electron-emitting diagnostic radioisotopes as well as therapeutic radioisotopes emitting alpha and beta particles on a nano-scale measurement using Geant4-DNA simulation in the DNA molecule and to perform a comparison between the effects of diagnostic and therapeutic radioisotopes.

Materials and Methods

DNA model

In the present study, two geometric models of the DNA molecule were simulated to calculate the mean number of SSBs and DSBs. These two models are similar to the model used by Bernal and Liendo,[19] Raisali *et al*.,[20] and Semsarha *et al*.,[21] [Figure 1], with the difference that each phosphate-sugar group is in the spherical shape (Model No. 1), and parallelepiped shape (Model No. 2). The two models are indicated in Figures 2 and 3. The geometric model of the DNA molecule considered by Raisali *et al*.,[20] consists of 41 bp (Base pair) (82 nucleotides) with ^{123}I atom being located in 21st bp. This position is the location of the IdUrd.

As shown in Figure 1, each sugar-phosphate group is simulated in volumes of height of 0.33 nm with an internal radius of 0.5 nm and an external radius of 1.185 nm. Each nucleotide contains a sugar-phosphate group and its related base, in such way that the volume of each sugar-phosphate group is 0.24 nm^3. This volume is the total volume of atoms of one sugar-phosphate group. All volumes are filled with water. Considering that the spiral of the DNA molecule spins 360° after 10 nucleotide pairs, an angle of 36° is intended to simulate the rotational angle for each nucleotide.

In this study, the new models were used considering the fact that the shape of phosphate-sugar groups can vary in different

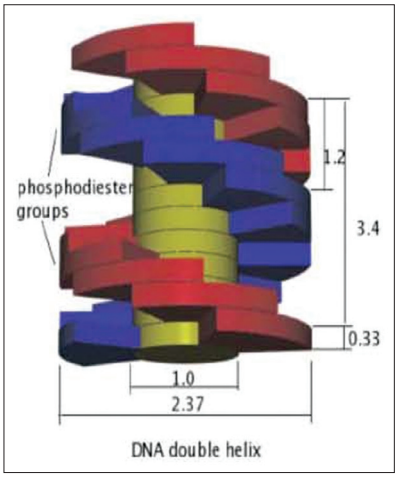

Figure 1: The volumetric model of the DNA molecule used by Bernal and Liendo,[17] Raisali *et al*.,[18] and Semsarha *et al*.,[19] (10 base pair of 41 base pair)

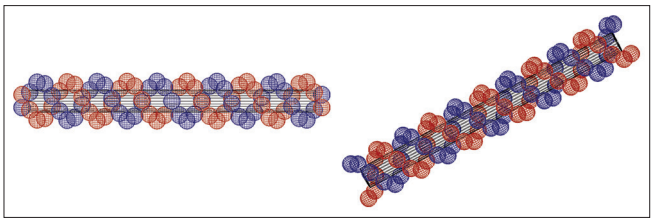

Figure 2: Volumetric model of the DNA molecule (spherical sugar- phosphate groups) (Model No. 1)

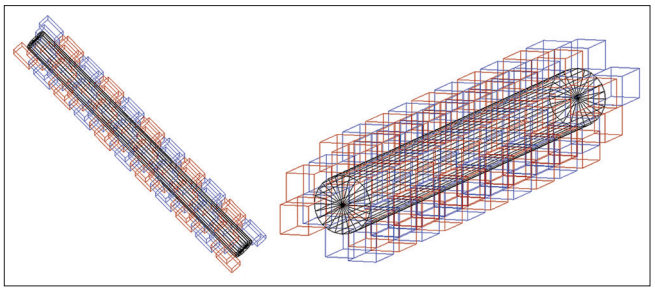

Figure 3: Volumetric model of the DNA molecule (parallelepiped sugar-phosphate group) (Model No. 2)

DNA molecules. Cylinders, spheres, and parallelepipeds was simulated with the same volume of 0.24 nm^3 used by Bernal and Liendo[19] and Raisali *et al*.,[20] (spherical radius: 0.385 nm and parallelepiped sides of: 0.5, 0.5, 0.96 nm and cylinder radius of 0.5 and height of 6.5 nm). The cylinder dimensions, which play the role of the axis of DNA molecule, are exactly the same dimensions used in previous studies Bernal and Liendo[19] and Raisali *et al*.[20] All volumes are placed inside an air-filled cube as world, with 10-μm sides.

A 10-micron side cube is large enough for the establishment of full scattering conditions, because the range of the low energy electrons is very low in water.

Both DNA molecule models consist of 41 bp (82 nucleotides). Each nucleotide contains a related sugar-phosphate group. The two models are shown in Figures 2 and 3. In the present study, two different models of DNA molecules were simulated to investigate the effect of the geometric shape of phosphate-sugar groups on DNA molecular breaks. All volumes were defined to be water-based. To define the physics of the problem, the physical model of G4EmDNAPhysics was used. Particle emissions were assumed to be isotropic.

Radioisotopes

Table 1 shows the average energy of emitted electrons in keV and their yield per decay for the nuclear medicine radionuclides used in simulation. Data of Table 1 are taken from the AAPM Nuclear Medicine Task Group Report.[27] Furthermore, Table 2 shows the average energy of emitted electrons and Alpha particles in keV and their yield per decay for the therapeutic radionuclides of ^{131}I (beta + Auger + CK emitter) and ^{211}At (alpha + Auger + CK emitter)[28-30]

Considering the low energy and short range of the Auger electrons, the radioisotope intracellular position is very important in calculating their dose rate.[31] In practice, radioisotope atoms are placed in 21st bp position at a distance of 0.57 nm from the central axis. The distance between the ^{125}I atom in ^{125}IdUrd and the central axis of DNA was estimated as 0.57 nm by Chen *et al*.,.[26] Raisali *et al*.,[20] also considered this position for radioisotopes and in order to make a comparison, the same position was selected in the present study too.

Calculations of DNA chain breaks

Due to the interactions of ionizing rays-DNA molecule, various DNA molecule damages occur. In order to determine the number of breaks, the present study investigated the energy absorption in sugar-phosphate volume. Thus, if energy absorbed in the sugar-phosphate group of the DNA molecule is more than the threshold energy value, a break will occur in the DNA molecule chain. This break is called SSB. If the distance between the two SSBs located on the two chains running opposite to each other, is less than the threshold value, then it is considered as a DSB. In this study, the threshold values for SSB and DSB due to direct and indirect effects of DNA molecules was selected similar to the threshold values used by Raisali *et al*.,[20] and Bernal and Liendo[19] and Pomplun.[7] The threshold energy value for SSB due to direct effects was 10.79 eV (This is the first energy ionization of the water molecule defined in the Geant4 Interaction Library, i.e., the threshold energy for detaching the electron from the 1b1 layer) and the threshold energy value for SSB due to indirect effects was 17eV. On average, this energy value is required to produce a radical pair in water.[32] In addition, the threshold distance between two SSBs for being scored as a DSB was considered to be 10 bp.

Given that the simulated DNA molecule has 41 bp and the Auger electrons range is short, the very small threshold distance (<10 bp), results in a significant reduction in the number of DSBs, and a very large threshold (>10 bp) does not have a significant effect on the number of DSBs.

On how to calculate SSBs or DSBs, according to Table 1 and 2, separately, SSB or DSB for each process, per decay were calculated, then multiplied by the respective yield and eventually the sum of SSBs or DSBs of all the processes were calculated. This is the final reported value of SSB and DSB for each radioisotope.

Results and Discussion

Calculation of single-strand breaks and double-strand breaks

The results of calculating SSB and DSB caused by the direct and indirect effects for the six commonly used diagnostic radioisotopes of $^{99\ m}Tc$, ^{67}Ga, ^{201}Tl, ^{111}In, ^{123}I, and ^{125}I, as well as the two therapeutic radioisotopes of ^{131}I (beta + Auger + CK emitter) and ^{211}At (alpha + Auger + CK emitter) are presented in Tables 3 and 4, respectively. These results are calculated from average of 10,000 decays and reported for one decay.

Table 1: The average energy of emitted electrons in keV and their yield per decay for the diagnostic radionuclides used in the Monte Carlo-based simulation[27]

^{67}Ga			^{111}In			^{125}I		
Process	**Ei**	**ni**	**Process**	**Ei**	**ni**	**Process**	**Ei**	**ni**
CK MMX	0.0624	2.07	CK NNX	0.0388	2.54	CK NNX	0.0299	3.51
CL LLX	0.0729	0.346	CK MMX	0.125	0.915	Auger NXY	0.0324	10.9
Auger LMM	0.921	1.68	CK LLX	0.183	0.151	CK MMX	0.127	1.44
Auger LMX	0.953	0.0116	Auger MXY	0.350	2.09	CK LLX	0.219	0.264
Auger KLL	7.43	0.470	Auger LMM	2.59	0.835	Auger MXY	0.461	3.28
Auger KLX	8.44	0.116	Auger LMX	3.06	0.190	Auger LMM	3.05	1.25
Auger KXY	9.46	0.0082	Auger LXY	3.53	0.0109	IC 1 K	3.65	0.191
IC 2 K	81.6	0.0027	Auger KLL	19.1	0.103	Auger LMX	3.67	0.340
IC 1 K	83.7	0.270	Auger KLX	22.3	0.0394	Auger LXY	4.34	0.0211
IC 1 L	92.2	0.0376	Auger KXY	25.5	0.0036	Auger KLL	22.4	0.138
IC 1 M, N	93.2	0.0066	IC 1 K	145	0.0824	Auger KLX	26.4	0.059
IC 3 K	175	0.0034	IC 1 L	167	0.01	Auger KXY	30.2	0.0065
IC 5 K	291	0.001	IC 1 M, N	171	0.0014	IC 1 L	30.6	0.110
			IC 2 K	219	0.0521	IC 1 M, N	34.1	0.0284
			IC 2 L	241	0.0091			
			IC 2 M, N	245	0.0019			
^{201}Tl			^{99}mTc			^{123}I		
Process	**Ei**	**ni**	**Process**	**Ei**	**ni**	**Process**	**Ei**	**ni**
Auger OXY	0.0161	17.6	CK NNX	0.0334	1.98	CK NNX	0.0298	2.10
CK OOX	0.0453	2.84	CK LLX	0.0429	0.0193	Auger NXY	0.0325	6.54
Auger NXY	0.0644	7.93	CK MMX	0.116	0.747	CK MMX	0.127	0.869
CK NNX	0.172	4.41	Auger MXY	0.226	1.10	CK LLX	0.213	0.156
CK MMX	0.406	0.923	IC 1 M, N	1.82	0.991	Auger MXY	0.461	1.97
CK LLX	0.773	0.322	Auger LMM	2.05	0.0868	Auger LMM	3.04	0.751
IC 1 M, N	0.895	0.608	Auger LMX	2.32	0.0137	Auger LMX	3.66	0.202
Auger MXY	1.83	2.03	Auger LXY	2.66	0.0012	Auger LXY	4.28	0.013
Auger LMM	7.58	0.541	Auger KLL	15.3	0.0126	Auger KLL	22.4	0.0838
Auger LMX	9.85	0.235	Auger KLX	17.8	0.0047	Auger KLX	26.3	0.0384
Auger LXY	12.0	0.0195	IC 2 K	119	0.0843	Auger KXY	30.2	0.0035
IC 2 L	12.2	0.0022	IC 3 K	122	0.0059	IC 1 K	127	0.130
IC 3 L	15.9	0.0861	IC 2 L	137	0.0136	IC 1 L	154	0.0179
IC 4 L	17.4	0.0724	IC 3 L	140	0.0062	IC 1 M, N	158	0.0053
IC 3 M, N	27.7	0.0236						
IC 4 M, N	29.4	0.0237						
IC 5 K	52.2	0.0797						
Auger KLL	55.0	0.0268						
Auger KLX	66.3	0.0153						
Auger KXY	77.5	0.0015						
IC 6 K	82.8	0.0025						
IC 7 K	84.3	0.159						
IC 5 L	121	0.0152						
IC 5 M, N	133	0.0027						
IC 7 L	153	0.0269						
IC 7 M, N	165	0.0094						

The selection of 10,000 decays per simulation was sufficient to ensure that the relative standard deviation of the results is <1%.

The mean difference between SSBs and DSBs of Model No. 1 (spherical) and Model No. 2 (parallelepiped) for the eight radioisotopes is equal to 16.87% and 25.75%, respectively. This difference is due to the effect of different geometric shapes used in both models. Considering the calculated SSBs and DSBs [Table 3], the following inequalities can be written for the above radioisotopes:

Spherical model:

SSB values ^{201}Tl $>^{125}$I $>^{211}$At $>^{123}$I $>^{111}$In $>^{99\ m}$Tc $>^{67}$Ga $>^{131}$I

DSB values ^{125}I $>^{201}$Tl $>^{123}$I $>^{211}$At $>^{111}$In $>^{99\ m}$Tc $>^{67}$Ga $>^{131}$I

Table 2: The average energy of emitted electrons and alpha particles in keV and their yield per decay for the therapeutic radionuclides of ^{131}I (beta + Auger + CK emitter) and ^{211}At (alpha + Auger + CK emitter)[28-30]

^{131}I			^{211}At		
Process	**Ei**	**ni**	**Process**	**Ei**	**ni**
CK NNX	0.0362	0.363	CK NNX	0.178	1.13
CK MMX	0.124	0.0446	CK MMX	0.442	0.277
CK LLX	0.318	0.0082	CK LLX	1.15	0.0909
Auger MNN	0.61	0.0057	Auger MXY	2.11	0.72
Auger MNX	0.76	0.00003	Auger NXY	0.109	2.08
Auger MXY	0.50	0.0997	Auger LMM	8.67	0.175
Auger LMM	3.32	0.0393	Auger LMX	11.3	0.0823
Auger LMX	4.00	0.0117	Auger LXY	14.00	0.0091
Auger LXY	4.70	0.0008	Auger OOX	0.0384	1.63
Auger NXY	0.0262	0.119	Auger OXY	0.127	0.0052
Auger KLL	24.5	0.0039	Auger KLL	63.5	0.0097
Auger KLX	28.7	0.0017	Auger KLX	76.7	0.0056
Auger KXY	32.9	0.0001	Auger KXY	86.8	0.00074
β	606.00	0.8930	α	6790.00	1.000

Table 3: Average number of single-strand breaks and double-strand breaks per decay caused by the direct effects of the auger electrons, beta and alpha particles for six diagnostic radioisotopes and the two therapeutic radioisotopes for two different geometric models of sugar-phosphate groups

Radionuclide	Model number 1 (spherical)	Model number 2 (parallelepiped)
111In Geant4-DNA		
SSB	0.87	0.66
DSB	0.28	0.17
67Ga Geant4-DNA		
SSB	0.51	0.53
DSB	0.12	0.22
201Tl Geant4-DNA		
SSB	2.84	3.63
DSB	0.75	0.58
99mTC Geant4-DNA		
SSB	0.55	0.40
DSB	0.21	0.17
123I Geant4-DNA		
SSB	1.29	1.27
DSB	0.56	0.57
125I Geant4-DNA		
SSB	2.14	2.14
DSB	0.93	0.95
131I Geant4-DNA		
SSB	0.06	0.06
DSB	0.02	0.02
211At Geant4-DNA		
SSB	1.51	0.75
DSB	0.45	0.28

SSB: Single-strand breaks, DSB: Double-strand breaks

Parallelepiped model:

SSB values ^{201}Tl $>^{125}$I $>^{123}$I $>^{211}$At $>^{111}$In $>^{67}$Ga $>^{99\ m}$Tc $>^{131}$I

DSB values ^{125}I $>^{201}$Tl $>^{123}$I $>^{211}$At $>^{67}$Ga $>^{99m}$Tc $>^{111}$In $>^{131}$I

Considering the above inequalities, ^{201}Tl and ^{125}I have had the greatest rate of SSBs and DSBs per decay in both simulation models. Also, $^{99\ m}$Tc and ^{67}Ga, among the diagnostic radioisotopes had the least effect. According to the emission spectrum of the studied radioisotopes [Table 1], ^{201}Tl and ^{125}I had the highest decay yields (38 and 21.5 electron per decay), respectively. As shown in Table 2, ^{131}I had the lowest decay yields (1.59 electron per decay). It should be noted that in addition to decay yields, the amount of particles energy also influences the breaks rate. For example, ^{211}At has low decay yields (6.21 electron per decay) but the proper energy of its electrons and alpha particles, caused a moderate impact on the breaks rate.

The mean energy of particles emitted from ^{125}I is less than that of ^{201}Tl, which results in the absorption of ^{125}I electrons at shorter distances than those emitted from ^{201}Tl in the sugar-phosphate group of the DNA molecule, which in turn leads to higher DSBs for ^{125}I in comparison with ^{201}Tl.

The ^{131}I therapeutic radioisotope almost did not have any effect on the SSBs and DSBs in both models, and the ^{211}At therapeutic alpha-emitting radioisotope had a moderate effect in this regard. This reveals the significance of dosimetry calculation and the study of the effects of the Auger electron-emitting diagnostic radioisotopes. Table 5 shows the results of studies previously carried out by Raisali *et al*.,[20] Pomplun[7] and Ftacnikova and Bohm[15] who calculated the SSBs and DSBs caused by the Auger electrons for ^{123}I and ^{125}I radioisotopes.

The SSBs and DSBs calculated by Raisali *et al*.,[20] Pomplun[7] and Ftacnikova and Bohm[15] are lower than those obtained in the present study [Table 3], which may be attributed to differences in calculation methods:

i. The volume of the sugar-phosphate groups proposed in the present study was equal to the same volume considered by Raisali *et al*.;[20] so, different geometric shapes of sugar-phosphate group can be considered as a factor leading to the difference in results. The effect of the sugar-phosphate group geometric shape varies in different energies, and this comparison demonstrates the importance of the effect of the geometric shape on the breaks of DNA molecules
ii. Differences in the radioisotope emission spectrum. For example, in the spectrum used for ^{123}I and ^{125}I radioisotopes Raisali *et al*.,[20] the yield per decay is considered to be 2.26 and 8.12, respectively, for Auger NXY electrons; however, the same values were reported to be 6.54 and 10.9 in the case of the spectrum used in the present study
iii. Differences in the simulation code (MOCA8b and ETRACK), the difference in the threshold energy value of SSBs (17.6 eV), and the different position of radioisotopes

are considered as the main reasons for the difference between the results.

Comparison of ^{123}I and ^{125}I radioisotopes showed that the mean SSB and DSB values of the ^{125}I in the spherical model were respectively 1.65 and 1.66 times more effective than ^{123}I, and in cubic model were 1.68 and 1.66 times more effective than the ^{123}I radioisotope. Raisali *et al*.,[20] (cylindrical model) reported that the mean of SSB and DSB values of ^{125}I radioisotope are 1.5 times more effective than ^{123}I. Also, the β-particles of ^{131}I, due to their energy and high range, had not any effect on the SSB and DSB of the DNA molecule.

The mean difference between SSBs and DSBs of Model No. 1 (spherical) and Model No. 2 (parallelepiped) for 8 radioisotopes is equal to 15.07% and 22.63%, respectively.

For all the radioisotopes, for both geometric models, the number of breaks caused by indirect effects is less than direct effects, and even the number of DSBs caused by indirect effects for most of the radioisotopes is zero. The lower the number of breaks due to indirect effects than direct effects is naturally due to the higher threshold that is considered for breaks by indirect effects. Considering the calculated SSBs and DSBs [Table 4], the following inequalities can be written for the above radioisotopes:

Spherical model:

SSB values ^{125}I $>^{201}$Tl $>^{211}$At $>^{123}$I $>^{111}$In $>^{67}$Ga $>^{99\ m}$Tc $>^{131}$I

DSB values ^{125}I $>^{201}$Tl $>^{211}$At $>^{123}$I $=^{111}$In $=^{67}$Ga $=^{99\ m}$Tc $=^{131}$I

Parallelepiped model:

SSB values ^{125}I $>^{201}$Tl $>^{123}$I $>^{211}$At $>^{111}$In $>^{99\ m}$Tc $>^{67}$Ga $>^{131}$I

DSB values ^{211}At $>^{125}$I $>^{201}$Tl $>^{123}$I $=^{111}$In $=^{67}$Ga $=^{99\ m}$Tc $=^{131}$I

Considering the above inequalities, ^{125}I almost in both simulation models has the greatest impact on the number of SSBs and DSBs due to indirect effects. Considering the total effects of direct and indirect [Tables 3 and 4], ^{201}Tl and ^{125}I, had the greatest impact on the number of SSBs and DSBs, respectively.

Considering the threshold of DNA molecule chain breaks to induce cell death,[12] we can evaluate the effects of cellular death induced by the Auger electrons of the widely used diagnostic radioisotopes. For example, ^{125}I, as one of the most effective radioisotopes on the DNA molecule chain breaks, leads to an average SSB and DSB number of 3.45 and 1.11 per decay [Table 6], respectively (in the spherical model). Therefore, a total of more than 43,000 decay of this radioisotope should occur to reach the threshold value for the induction of cell death as apoptosis. This conclusion has been made using a few approximations, and considering the repair potential in different cells, this conclusion needs to be corrected. To achieve definitive results, further calculations and laboratory researches need to be carried out on the rate of SSBs and DSBs of the DNA molecule caused by the Auger electron of the diagnostic radioisotopes.

Table 4: Average number of single-strand breaks and double-strand breaks per decay caused by the indirect effects of the Auger electrons, beta and alpha particles for six diagnostic radioisotopes and the two therapeutic radioisotopes for two different geometric models of sugar-phosphate groups

Radionuclide	Model number 1 (spherical)	Model number 2 (parallelepiped)
111In Geant4-DNA		
SSB	0.48	0.43
DSB	0	0
67Ga Geant4-DNA		
SSB	0.30	0.21
DSB	0	0
201Tl Geant4-DNA		
SSB	1.22	0.88
DSB	0.14	0.01
99mTC Geant4-DNA		
SSB	0.22	0.22
DSB	0	0
123I Geant4-DNA		
SSB	0.74	0.69
DSB	0	0
125I Geant4-DNA		
SSB	1.31	1.15
DSB	0.17	0.02
131I Geant4-DNA		
SSB	0.03	0.02
DSB	0	0
211 at Geant4-DNA		
SSB	0.80	0.55
DSB	0.10	0.10

SSB: Single-strand breaks, DSB: Double-strand breaks

Validation of simulation results

Among the diagnostic and therapeutic radioisotopes located on the base thymidine position of the 21st bp of DNA molecule, only the SSBs and DSBs of the ^{125}I radioisotope (as ^{125}IdUrd radiopharmaceutical) have been investigated *in vitro*.[33] IdUrd is a radiopharmaceutical that carries ^{123}I or ^{125}I and is located on the base thymidine position of the DNA molecule. The number of SSBs and DSBs was not measured directly in case of ^{123}I radioisotope (as ^{123}IdUrd radiopharmaceuticals).

Thus, out of the radioisotopes that are simulated in this study, only the simulation results of the ^{125}I, a diagnostic radioisotope, can be compared with experimental results. This position (21st bp of DNA molecule) was selected in the present research so as to compare the results with the results of Raisali *et al.*'s research,[20] in which the same position was also selected. Another reason for choosing such position for the remaining radioisotopes, regardless of the possibility of labeling the above radioisotopes with the above drug, was simply to select the same position for all radioisotopes in order to compare their effects on the molecular chain breaks. Overall, it can be stated that the simulation results of these diagnostic and therapeutic

Table 5: The mean number of single-strand breaks and double-strand breaks caused by the direct effects of the Auger electrons per decay of the two radioisotopes of ^{123}I and ^{125}I, calculated by Raisali *et al*.,[18], Pomplun[7] and Ftacnikova and Bohm[15]

Radionuclide	Damage	Raisali *et al*.,[18] (Geant4-DNA)	Pomplun.[7] MOCA8b	Ftacnikova and Bohm[15] ETRACK
^{123}I	SSB	1.10	1.1	0.72
	DSB	0.29	0.2	-
^{125}I	SSB	1.68	1.9	1.18
	DSB	0.69	0.4	0.73

SSB: Single-strand breaks, DSB: Double-strand breaks, MOCA: Monte Carlo

Table 6: Number of mean single-strand breaks and double-strand breaks caused by the direct and indirect effects of ^{125}I auger electrons calculated by Geant4-DNA, and a comparison with Raisali *et al*.,[18] as well as experimental results[33]

	This study (model number 1: spherical)	This study (model number 2: parallelepiped)	Raisali *et al*., 2013 (Geant4-DNA)	LeMotte and Little 1984 (experimental data)
SSB (direct)	2.14	2.14	1.68	-
SSB (indirect)	1.31	1.15	1.45	-
SSB (all)	3.45	3.29	3.13	4.3
DSB (direct)	0.93	0.95	0.69	-
DSB (indirect)	0.17	0.02	0.44	-
DSB (all)	1.11	0.97	1.13	0.86

SSB: Single-strand breaks, DSB: Double-strand breaks

radioisotopes can provide useful information to achieve a better understanding of their effects on DNA molecule. Also, if these radioisotopes are labeled with the above drug (IdUrd) in the future, the results of this research will be valuable.

LeMotte and Little[33] measured the number of ^{125}I–induced SSBs and DSBs in human diploid fibroblasts using experimental methods.

Table 6 shows the results of total SSBs and DSBs induced by direct and indirect effects obtained in this study, the results of Raisali *et al*.,[20] together with the experimental results of LeMotte and Little.[33]

The data presented in Table 6 show that the simulation results of both models No. 1 and 2 are almost in good agreement with the simulation results of Raisali *et al*.,[20] and the experimental results of LeMotte and Little.[33] Roots *et al*.,[34] also suggested that the measured values by LeMotte and Little[33] should be reduced by 30% to correct the number of SSBs measured by this experimental method. Thus, the number of SSBs would be equal to 3.01 accordingly and our results would be in better agreement with the SSBs of the experimental results.

Conclusion

The aim of the present study was to conduct a comprehensive assessment on the effects of widely-used diagnostic nuclear medicine radioisotopes as well as therapeutic radioisotopes on a nano-scale measurement using Geant4-DNA simulation. The present study investigated the effects of these radioisotopes on SSBs and DSBs in the DNA molecule. The results showed that ^{201}Tl and ^{125}I had the maximum effect on DNA by inducing number of SSBs and DSBs, while the therapeutic radioisotope of ^{131}I (beta + Auger + CK emitter) almost had no effect on the rate of induction of strand breaks and therapeutic radioisotope of ^{211}At (alpha + Auger + CK emitter) had the moderate effect. These results demonstrated the importance of performing nanoscale dosimetry calculation on these diagnostic radioisotopes, and also prove the potential of using these radioisotopes in the radiation therapy. In this study, two models with two different shapes of sugar-phosphate group were simulated to investigate the effect of geometric shape of sugar-phosphate groups on the rate of DNA SSBs and DSBs. The results of the two models were also compared with each other as well as with the results of others. The results revealed that different geometric shapes of sugar-phosphate groups could have a significant effect on the rate of SSBs and DSBs, even if the sugar-phosphate groups were considered to be of the same volume.

Financial support and sponsorship

Nil.

Conflicts of interest

There are no conflicts of interest.

References

1. Kassis AI, Adelstein SJ. Radiobiologic principles in radionuclide therapy. J Nucl Med 2005;46 Suppl 1:4S-12S.
2. Howell RW. Auger processes in the 21st century. Int J Radiat Biol 2008;84:959-75.
3. Pool SE, Krenning EP, Koning GA, van Eijck CH, Teunissen JJ, Kam B, *et al*. Preclinical and clinical studies of peptide receptor radionuclide therapy. Sem Nucl Med 2010;40:209-18.
4. Rebischung C, Hoffmann D, Stefani L, Desruet MD, Wang K, Adelstein SJ, *et al.* First human treatment of resistant neoplastic meningitis by intrathecal administration of MTX plus (125) IUdR. Int J Radiat Biol 2008;84:1123-9.

5. Vallis KA, Reilly RM, Scollard D, Merante P, Brade A, Velauthapillai S, *et al*. Phase I trial to evaluate the tumor and normal tissue uptake, radiation dosimetry and safety of (111) In-DTPA-human epidermal growth factor in patients with metastatic EGFR-positive breast cancer. Am J Nucl Med Mol 2014;4:181-92.
6. Stigbrand T, Carlsson J, Adams G, Targeted Radionuclide Tumor Therapy. 1st ed. Netherlands: Springer; 2008.
7. Pomplun E. 123I: Calculation of the auger electron spectrum and assessment of the strand breakage efficiency. AAPM Symp Ser 1992;8:121-36.
8. Watanabe N, Sawai H, Ogihara-Umeda I, Tanada S, Kim EE, Yonekura Y, *et al.* Molecular therapy of human neuroblastoma cells using auger electrons of 111In-labeled N-myc antisense oligonucleotides. J Nucl Med 2006;47:1670-7.
9. Faraggi M, Gardin I, Labriolle C, Moretti J, Bok B. The influence of tracer localization on the electron dose rate delivered to the cell nucleus. J Nucl Med 1994;35:113-9.
10. Joiner M, Kogel A. Basic Clinical Radiobiology. 4th ed. Florida, USA: Hodder Arnold; 2009.
11. Khan FM, Treatment Planning in Radiation Oncology. 2nd ed. Baltimore: Lippincott Williams and Wilkins; 2007.
12. Tounekti O, Kenani A, Foray N, Orlowski S, Mir LM. The ratio of single- to double-strand DNA breaks and their absolute values determine cell death pathway. Br J Cancer 2001;84:1272-9.
13. Nikjoo H, Goodhead DT, Charlton DE, Paretzke HG. Energy deposition in small cylindrical targets by ultrasoft X-rays. Phys Med Biol 1989;34:691-705.
14. Charlton DE, Humm JL. A method of calculating initial DNA strand breakage following the decay of incorporated 125 I. Int J Radiat Biol 1988;53:353-65.
15. Ftacnikova S, Böhm R. Monte carlo calculations of energy deposition in DNA for auger emitters. Radiat Prot Dosim 2000;92:269-78.
16. Humm JL, Charlton DE. A new calculational method to assess the therapeutic potential of auger electron emission. Int J Radiat Oncol Biol Phys 1989;17:351-60.
17. Friedland W, Jacob P, Paretzke HG, Stork T. Monte Carlo simulation of the production of short DNA fragments by low –linear energy transfer radiation using higher –order DNA models. Radiat Res 1998;150:170-82.
18. Friedland W, Dingfelder M, Kunderat P, Jacob P. Track structures, DNA targets and radiation effects in the biophysical Monte Carlo simulation code PARTRAC. Mutat Res 2011;711:28-40.
19. Bernal MA, Liendo JA. An investigation on the capabilities of the Penelope MC code in nanodosimetry. Med Phys 2009;36:620-5.
20. Raisali GH, Mirzakhanian L, Masoudi SF, Semsarha F. Calculation of DNA strand breaks due to direct and indirect effects of auger electrons from incorporated 123 I and 125 I radionuclides using the geant4 computer code. Int J Radiat Biol 2013;89:57-64.
21. Semsarha F, Raisali GR, Goliaei B, Khalafi H. Study of strand breaks induced by direct effects of monoenergetic electrons in B conformation of genetic material of living cells by using Geant4. J Nucl Sci Technol 2015;71:51-9.
22. Kim JY, Park HC, Kim SJ, Chang HS, Choi HJ, Kim YH, *et al.* Assessment of left ventricular ejection fraction by thallium-201 myocardial SPECT-CT in patients with angina pectoris: Comparison with 2D echocardiography. Nucl Med Mol Imaging 2019;53:136-43.
23. Gabilondo I, Llorens V, Rodriguez T, Fernandez M, Concha T, Acera M. Myocardial MIBG scintigraphy in genetic Parkinson's disease as a model for Lewy body disorders. Eur J Nucl Med Mol Imaging 2019;46:376-84.
24. Farzin L, Sheibani S, Moassesi ME, Shamsipur M. An overview of nanoscale radionuclides and radiolabeled nanomaterials commonly used for nuclear molecular imaging and therapeutic functions. J Biomed Mater Res A 2019;107:251-85.
25. Tseng JR, Chang Y, Yang L, Wu CT, Chen SY, Wan CH, *et al*. Potential usefulness of 68Ga-citrate PET/CT in detecting infected lower limb prostheses. Eur J Nucl Med Mol Imaging 2019;9:1-8.
26. Chen K, Adelstein SJ, Kassis AI. Molecular simulation of ligand-binding with DNA: Implications for 125I-labeled pharmaceutical design. Int J Radiat Biol 2004;80:921-6.
27. Howell RW. Radiation spectra for auger-electron emitting radionuclides: Report no. 2. AAPM Nuclear Medicine Task Group No. 6. Med Phys 1992;19:1371-83.
28. Stepanek J, Larsson B, Weinrei R. Auger –electron spectra of radionuclides for therapy and diagnostic. Acta Oncol 1996;35:863-8.
29. Adriana Alexandre S, Tavares A, João Manuel RS. Evaluating 99mTc Auger electrons for targeted tumor radiotherapy by computational methods. Med Phys 2010;37:3551-9.
30. Josefsson A. Microdosimetry of radiohalogens in thyroid models. Department of Radiation Physics. Institute of Clinical Sciences. Sahlgrenska Academy at University of Gothenburg; 2014.
31. Roeske JL, Aydogan B, Bardi`es M, Humm JL. Small-scale dosimetry: Challenges and future directions. Semin Nucl Med 2008;38:367-83.
32. Chatterjee A, Magee JL. Theoretical investigation of the production of strand breaks in DNA by water radicals. Radiat Prot Dosim 1985;13:137-40.
33. LeMotte PK, Little JB. DNA damage induced in human diploid cells by decay of incorporated radionuclides. Cancer Res 1984;44:1337-42.
34. Roots R, Kraft G, Gosschalk E. The formation of radiation-induced DNA breaks: The ratio of double-strand breaks to single-strand breaks. Int J Radiat Oncol Biol Phys 1985;11:259-65.